State-Resolved Dynamics of Dissociation of Triplet Acetaldehyde: Rate of Appearance of Fragment HCO and Decay of Excited States of Parent Molecule†

Cheng-Liang Huang,‡ Volume Chien,‡ Chi-Kung Ni,§ A. H. Kung,§ and I-Chia Chen*,‡

Department of Chemistry, National Tsing Hua University, Hsinchu, Taiwan 300, Republic of China, and Institute of Atomic and Molecular Sciences, Academia Sinica, P.O. Box 23-166, Taipei, Taiwan 106, Republic of China

Received: February 7, 2000; In Final Form: June 27, 2000

We studied the state-resolved dynamics of acetaldehyde in electronically excited state $\tilde{A}^1A''$ with high resolution, 0.025 cm^{-1}. Near a threshold for dissociation into $CH_3 + HCO$ that is 1500−1750 cm^{-1} above the vibrational ground state of acetaldehyde in $\tilde{A}^1A''$, the vibrational levels are investigated with laser-induced fluorescence. The rotational structures of four bands in this region are partially assigned. These assignments allow us to determine the dependence of relaxation of individual rovibrational levels on energy as well as rotational quantum number *J*. The measured lifetimes vary with *J* as a result of an increased number of nuclear hyperfine T_1 states that couple with a selected vibrationally excited state. For these four vibrational levels the rate constants of fragment HCO appearance are greater than decay for initially prepared excited states; this deviation implies that only a fraction of initially prepared states couple effectively to dissociation.

1. Introduction

The mechanisms of unimolecular dissociation of molecules at levels of vibrational excitation are of fundamental interest for understanding reaction dynamics and chemical reactivity. High-resolution spectra of excited molecules with diverse techniques of detection provide much information on coupling between various zero-order vibrational modes that typically control early stages of redistribution of vibrational energy and interaction among electronic surfaces when the electronically excited states are accessed.[1−14] When these states are correlated to dissociation channels, the spectroscopy provides a foundation for understanding of dissociation dynamics.

The transition $\tilde{A}^1A''-\tilde{X}^1A'$ of acetaldehyde is described as $n-\pi^*$. Upon excitation to state $\tilde{A}^1A''$, intersystem crossing to state T_1 and then to dissociation with an exit barrier for formation of $CH_3 + HCO$ is suggested to be the major pathway for dissociation.[15] We in this laboratory[16] and Gejo et al.[17] reported fluorescence decay of state $\tilde{A}^1A''$ with a quantum-beat phenomenon, attributed to interaction with state T_1. Because the triplet manifold is correlated to a dissociation continuum, near the top of dissociation barrier, states coupled to triplet manifold display short lifetimes.[16−18]

The lifetime of $J_{Ka} = 0_0$ of vibrational ground state of $\tilde{A}^1A''$ is reported to be 171 ns resulting mainly from internal conversion to the ground electronic state.[19] The rate of internal conversion is expected to increase with energy. Then, a large lifetime indicates mixing with character of triplet states. Mixing of states $\tilde{A}^1A''$ and T_1 increases with rotational quantum number *J* and is observed from increase of number of beat frequency in the quantum beat experiments.[17,18] This can be explained that the nuclear hyperfine states become more numerous as *J* increases.

At large excitation energy near the top of the dissociation barrier on the triplet surface, the molecule is expected to tunnel through the exit barrier to form products; therefore, the rate of decay of excited acetaldehyde is expected to increase from coupling to triplet states. In transformed plots of decay traces with quantum beats, the bandwidth increases with rotational quantum numbers *J* and *K*, indicating a systematic dependence on rotational quantum number for decay of the triplet states. A Coriolis-induced vibrational coupling within the triplet manifold to a dissociation continuum on the exit side of the dissociation barrier is proposed.[18]

Here we discuss use of a laser with high resolution in frequency and temporal domains to investigate relaxation and dissociation at a state-resolved level of detail. Near the top of the dissociation barrier on the triplet surface, in the region 1500−1750 cm^{-1} above the ground vibrational state of acetaldehyde in $\tilde{A}^1A''$, we recorded spectra with resolution 0.025 cm^{-1} and decay curves of individual states. The appearance of fragment HCO is detected when acetaldehyde is photolyzed at medium resolution 0.1 cm^{-1}. The state-resolved dynamics of dissociation is investigated from both the dissociation of the parent molecule and the appearance of fragments.

2. Experimental Section

1. High Resolution. As experimental details are described elsewhere[18] only a brief description is given here. Acetaldehyde (Aldrich 99.5%) seeded in helium 0.1−1% in a supersonic jet was detected with laser-induced fluorescence via transition $\tilde{A}^1A''-\tilde{X}^1A'$. The gas mixtures were expanded through an orifice (General Valve, diameter 0.2 mm) into a vacuum chamber with stagnation pressure 7−10 atm. The rotational temperature of acetaldehyde in the jet was estimated to be less than 2 K for a mixture at 0.1%.

A tunable beam from a UV laser was obtained by mixing the output at 532 nm from a seeded Nd:YAG laser (Spectra Physics, GCR 190) with the output of a pulsed amplifier in a

† Part of the special issue "C. Bradley Moore Festschrift".

* To whom all correspondence should be addressed. E-mail address: icchen@mx.nthu.edu.tw. Fax: 886-3-5721614.

‡ National Tsing Hua University.

§ Institute of Atomic and Molecular Sciences.

10.1021/jp000478p CCC: $19.00
Published on Web 08/12/2000

KDP crystal (INRAD, KDP-C). Output of the single-mode Ti-sapphire laser (Coherent 899-29) was used as a seeding beam for the pulsed amplifier. This amplifier pumped with a Nd:YAG laser contains the first stage of dye and the second stage of Ti:sapphire, pumped with another Nd:YAG laser, to yield pulses at energy 20−30 mJ/pulse and repetition rate 30 Hz. The output of the pulsed amplifier has a transform-limited bandwidth in wavelength range 780−794 nm and temporal width 4−5 ns. This laser system is described in detail elsewhere.[20,21] After frequency mixing the UV beam has an energy 2.5−3 mJ/pulse in a wavelength range 316−320 nm and bandwidth ∼100 MHz.

The total emission of acetaldehyde was collected through two lenses onto a photomultiplier without an amplifier; between the lenses a slit was set to limit the Doppler spectral width to ≤0.025 cm^{-1}. Decays of fluorescence of individual levels were recorded with a digital oscilloscope (Tektronix 744A, 500 MHz) and were averaged over 2000−3000 shots. Each trace is 1 μs long containing 500−1000 points with a step size of 1−2 ns. Some background curves were recorded by detuning the wavelength from acetaldehyde lines; these decay were fitted with Gaussian functions to give a full width at half-maximum (fwhm) around 7 ns.

2. Medium Resolution. Acetaldehyde in helium (0.6−2.5%) was expanded through a pulsed nozzle (General Valve, dia. 0.5 mm) operating at a repetition rate 10 Hz with a stagnation pressure 3−7 atm. The output of a dye laser (Continuum ND60, dual grating, DCM dye) pumped with a Nd:YAG laser (Continuum NY81-C) was directed to a KDP crystal to generate wavelength 330−350 nm with an energy 5−7 mJ/pulse and resolution 0.1 cm^{-1}. These laser pulses serve to excite acetaldehyde to state $\tilde{A}^1A''$. The region of excitation was selected for which rotational assignments are known and spectral transitions are resolved. The decay of acetaldehyde was recorded with a digital oscilloscope (Tektronix 620B, bandwidth 500 MHz) and about 1000 shots were averaged for each curve.

The detailed experimental setup for detection of fragment HCO is described elsewhere[15] and is summarized as follows. A second dye laser pumped with a Nd:YAG laser (Continuum NY82) generated pulses 10−15 mJ near wavelength 516 nm (dye Coumarin 500). The frequency was doubled in a BBO crystal to give a UV beam with energy 1.5−2.5 mJ/pulse to excite HCO to state $\tilde{B}^2A_1$ 0°. The wavelength of the probe beam was fixed either at the bandhead region or at transition $^QP_0(4)$. Both the photolysis and probe laser pulses overlapped spatially and interacted with the molecular jet 1.2−1.5 cm downstream from the orifice of the nozzle. Total fluorescence of formyl radical was detected with a photomultiplier (EMI 9658R) after interference filters (CVI, 334 ± 10 nm). The temporal delay between the photolysis and probe laser pulses was varied from −100 to 500 ns with step size 2 ns to produce a rise curve of HCO. The decay of excited acetaldehyde was recorded when the probe laser was turned off and other conditions were kept unaltered.

3. Results and Discussion

1. Spectra and Fluorescence Decay at High Resolution. The fluorescence excitation spectrum of acetaldehyde near the top of the dissociation barrier on the triplet surface was recorded. In this region, only small portion of spectrum is assigned because of its complicated spectral features. Many groups reported spectra and assignments of $\tilde{A}^1A''-\tilde{X}^1A'$ near the origin of $\tilde{A}^1A''$.[19,22−29] However, because the torsional motion of methyl and inversion of aldehyde hydrogen interact, definite assignments of vibrational and rotational levels at a vibrational energy near and above the torsional barrier ∼600 cm^{-1} remain unresolved. Rovibrational assignments including the interaction of torsional and rotational motions at energy near and above 600 cm^{-1} are currently under investigation. Hence, at energy of interest in the present work, the vibrational assignments are unavailable. Here we report vibrational bands near the top of dissociation barrier on the triplet surface with partial rotational

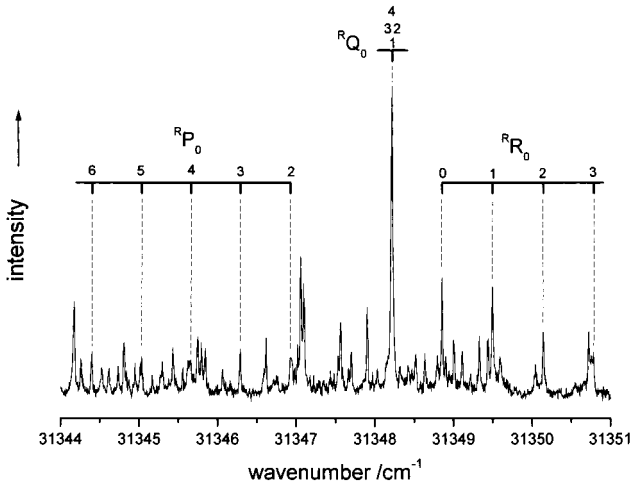

Figure 1. Spectrum and assignments of a band near its origin at 31 348 cm^{-1} of $\tilde{A}^1A''-\tilde{X}^1A'$ of acetaldehyde recorded with resolution 0.025 cm^{-1}.

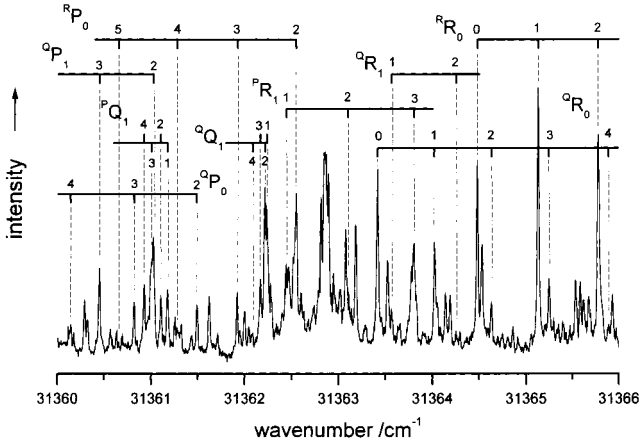

Figure 2. Spectrum and assignments of a band near its origin at 31 362 cm^{-1} of $\tilde{A}^1A''-\tilde{X}^1A'$ of acetaldehyde recorded with resolution 0.025 cm^{-1}.

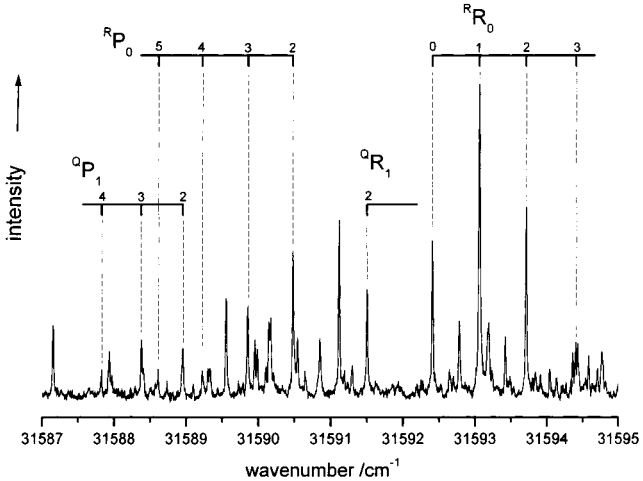

Figure 3. Spectrum and assignments of a band near its origin at 31 585 cm^{-1} of $\tilde{A}^1A''-\tilde{X}^1A'$ of acetaldehyde recorded with resolution 0.025 cm^{-1}.

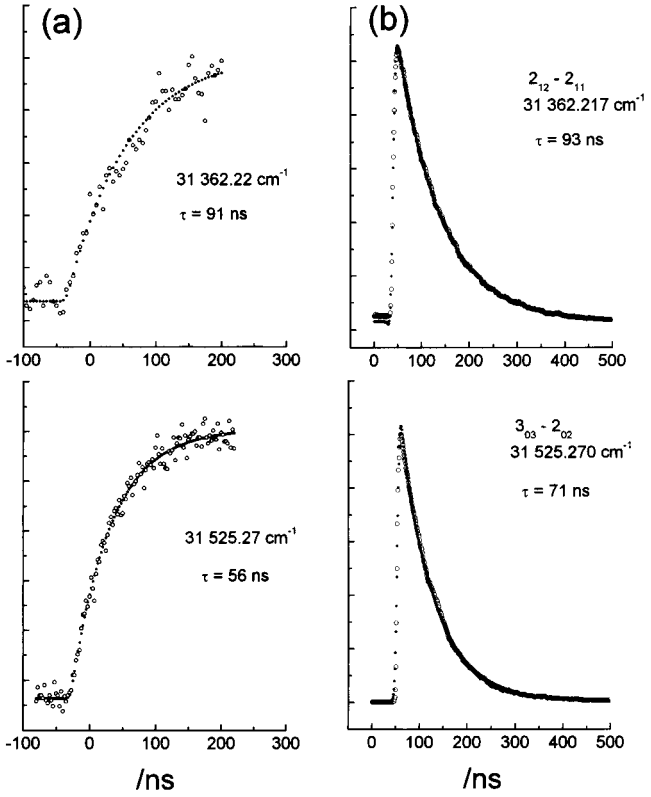

Figure 4. Experimental (open circles) and fitted (filled circles) curves of (a) appearance for fragment HCO and of (b) fluorescence decay for acetaldehyde denoted with excitation energy. The decay curves with assignments $J_{KaKc}' - J_{KaKc}''$ are recorded with high resolution and the rise curves with medium resolution. The fitted decay curves were convoluted with a Gaussian function with fwhm = 7 ns and the rise curves with a cross-correlated Gaussian function fwhm = 10 ns.

assignments and label them according to their band origin. The bands near origins 31 348, 31 362, and 31 585 cm^{-1} recorded at resolution 0.025 cm^{-1} and rotational assignments are displayed in Figures 1−3, respectively. The assignments and spectrum of another band in this region at 31 528 cm^{-1} are shown previously.[18] All rotational assignments were made according to the method of combinational differences of rotational levels in the ground electronic state; all assigned lines belong to the a−a torsional transition (components a and e resulted from torsional splitting). Some assignments were confirmed from having similar quantum-beat pattern in decay curves. The remaining unassigned lines can arise from states with large J and K, e torsional states or from other vibrational levels.

Fluorescence decays of rovibrational levels of $\tilde{A}^1A''$ in the same region were recorded; some experimental curves are shown in Figure 4. Most decays display more or less oscillatory modulation when excited with a high-resolution laser. For excitation with medium resolution, curves tend to display biexponential decay from superposition of more states. The fraction of levels showing beating modulation varies and there appears to be no systematic dependence on vibrational energy or on vibrational quantum number. Details of the beating phenomenon appear elsewhere.[16,18] Here we report the results of the rate of decay of individual excited states. All the decay curves were deconvoluted from the instrument response function to obtain accurate time constants. The overall instrument response was assumed to be a Gaussian function from fitting to some background traces measured experimentally. To compare the decay of all states we obtain time constants from best fits to exponential functions, even for curves with oscillatory modulation. Only few decay curves display large modulation and cannot be fitted exponentially.

In the region of interest in the present work, about 15−35% of curves display biexponential behavior and those are as shown in Figure 5; we assign the fast component to dephasing of eigenstates (or intersystem crossing) and the slow one to decay of eigenstates according to Lahmani et al.[30,31] and Kommandeur et al.[32−35] These eigenstates consist of mixture of the S_1 (bright) and T_1 (dark) states. Hence we use the time constant of the slow component to compare with that of the rise of fragment HCO.

We made fits for states in a frequency region 31 250−31 600 cm^{-1}; as the threshold for formation of radical products is estimated to be 31 650 cm^{-1},[36] this region about 50−400 cm^{-1} below is considered to be within the tunneling range for formation of radical products. The results of time constants (slow component only) obtained for all states detected versus excitation energy are displayed in Figure 6. According to this plot, within a vibrational level the decay time constant varies but the overall time decreases abruptly near 31 600 cm^{-1} consistent with the previously determined value for threshold. In this region there is near one band per 10−20 cm^{-1}. Toward lower energy, some states display long lifetimes, and the variation of the time

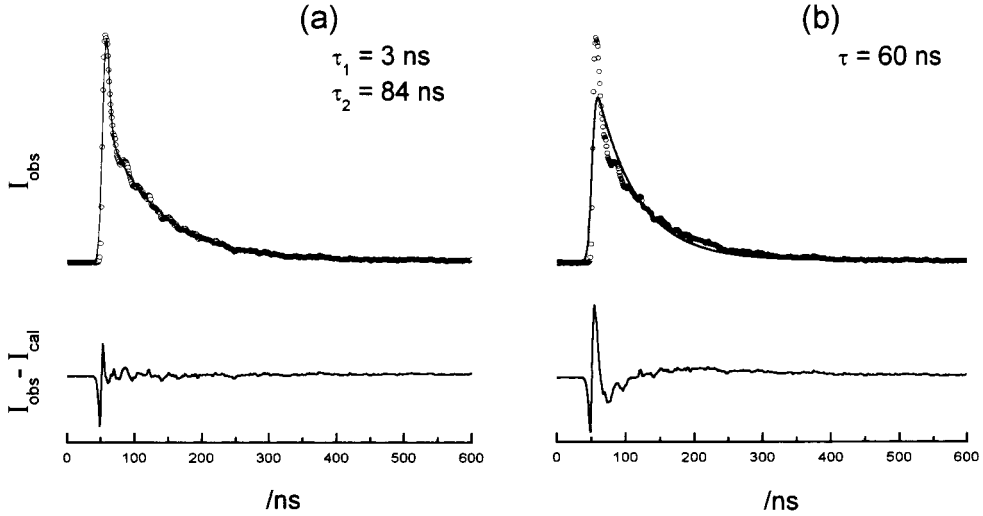

Figure 5. Experimental decay curve at excitation energy 31 524.004 cm^{-1} obtained at high resolution with best fit to (a) biexponential and (b) single exponential functions. Both fitted curves are convoluted with a Gaussian function with a fwhm = 7 ns.

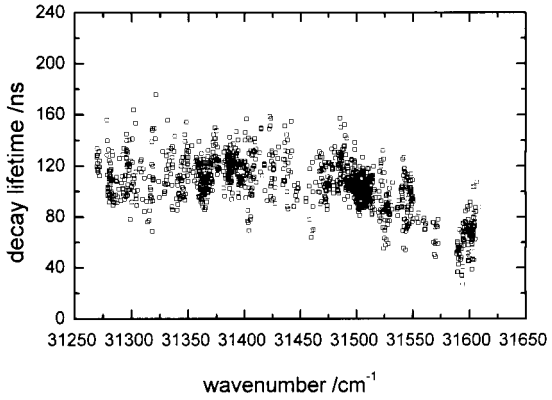

Figure 6. Plots of decay lifetime of $\tilde{A}^1A''$ state obtained at high resolution with best fit to an exponential function vs excitation energy; the time constant of the slow component is shown here when a biexponential function is used for fitting.

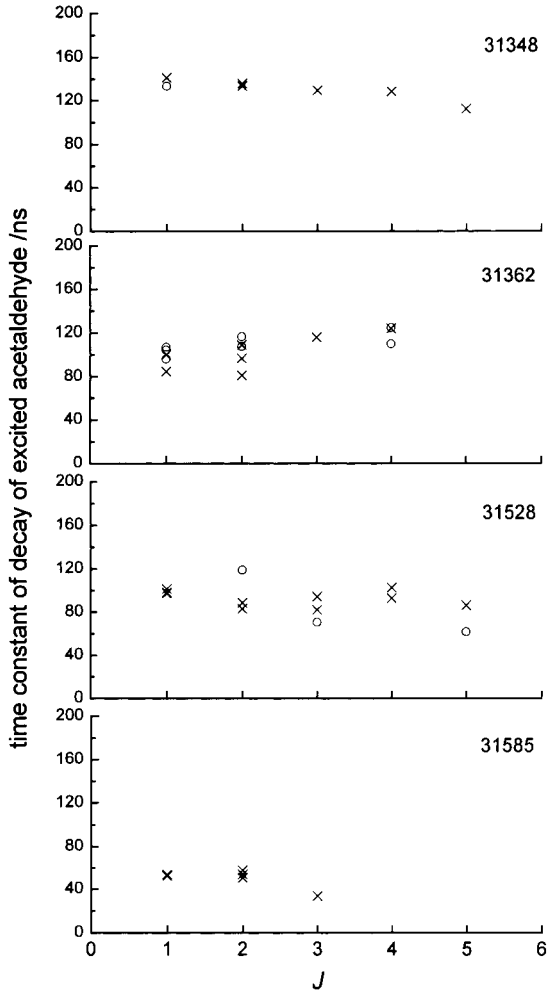

Figure 7. Plots of decay lifetime of $\tilde{A}^1A''$ state vs rotational quantum number J for levels near origins at 31 348, 31 362, 31 523, and 31 585 cm^{-1}. Symbol circle denotes state $K = 0$ and cross for $K = 1$.

constant for decay is smaller than for states near the dissociation threshold. At high energy the lifetime can be as small as ~20 ns. The fast components of biexponential fits corresponding to short dephasing time are from less than the uncertainty with the method of convolution (~2 ns) to 5 ns. Abou-Zied and McDonald[37] reported an evolution time constant around 665 ps for fragment HCO and CH_3CO from acetaldehyde at 266 nm photolysis; the intersystem crossing for S_1-T_1 is the rate-limiting step for dissociation. At the excitation energy we are

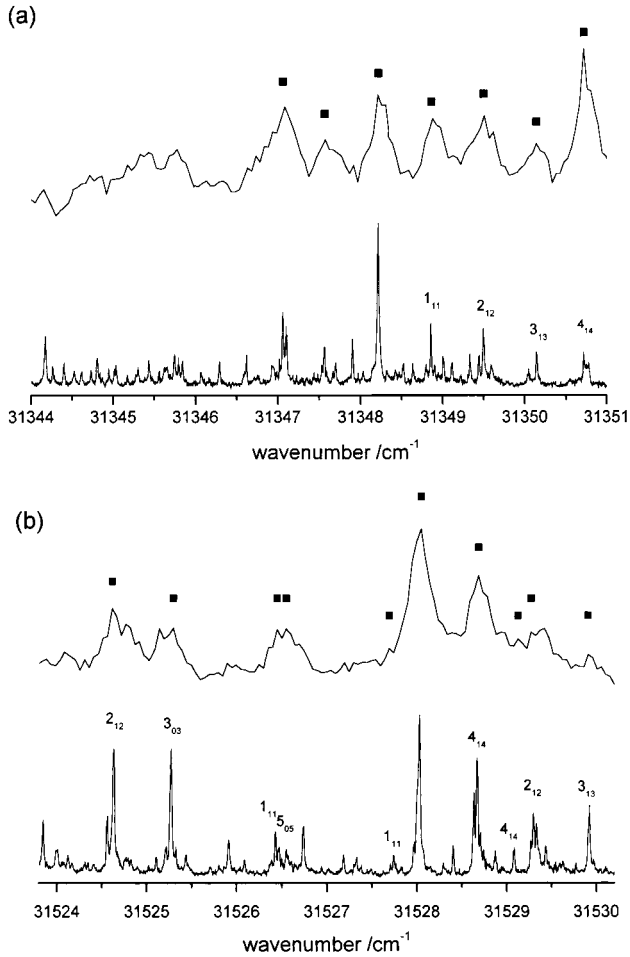

Figure 8. Spectra of fluorescence excitation of $\tilde{A}^1A''-\tilde{X}^1A'$ of acetaldehyde obtained at high (lower trace) and medium (upper trace) resolution for bands near (a) 31 348 and (b) 31 528 cm^{-1}; filled squares on the upper trace denote transitions used to detect the rise of fragment HCO. The assignment on the lower trace is J_{KaKc}'.

interested in in this work, a relatively slow intersystem crossing rate is expected; our values agree with the results of Abou-Zied and McDonald.[37] However, near the dissociation threshold the rate-limiting step is the formation of radical products.

Because some rotational states are assigned, we selected lines with little overlap to produce state-resolved lifetimes. The plot of the fitted time constant versus rotational quantum number J in Figure 7 for four vibrational levels facilitates comparison of their behavior. Near the top of dissociation barrier on the triplet surface the molecule is expected to tunnel through the exit barrier to form products. One would expect that lifetime decreases from mixing with more triplet states. Indeed the two levels at high energy show decreased lifetimes with increasing J. We would expect that the two states at low energy undergo tunneling less efficiently; an increase in lifetime is expected from coupling to more triplet states that are not dissociating. However, the level at 31 348 cm^{-1} has a short lifetime from coupling to more triplet states. This indicates that the triplet states coupled to this level may interact with the dissociation channel more efficiently than those to the level at 31 362 cm^{-1} that is 14 cm^{-1} higher in energy. This would imply a specificity of vibrational mode or symmetry for dissociation, as suggested by Choi and Moore for HFCO dissociation.[8,9] Another explanation is that the variation occurs from the process of internal conversion to the S_0 state. Noble and Lee[38] reported that the vibrational mode ν_{10} (CCO deformation) and ν_{14} (CH out-of-

TABLE 1: Time Constant for Rise HCO Rise and for Decay of Acetaldehyde in State $\tilde{A}^1A''$ [a]

	medium resolution			high resolution		
position/cm^{-1}	τ^{rise} /ns	τ_1^{decay}/ns	τ_2^{decay}/ns	τ_1^{decay}/ns	τ_2^{decay}/ns	transition
level 31 348						
31 346.920	126	11	121	<2	139	$1_{11}-2_{02}$
31 347.566	96	10	120		98	
31 348.213	135	12[b]	141[b]		154	$1_{11}-1_{01}$,$2_{12}-2_{02}$,$3_{13}-3_{03}$, $4_{14}-4_{04}$
31 348.850	122	11[b]	131[b]	5	141	$1_{11}-0_{00}$
31 349.328	137	10	131			
31 349.493	98	11	131		125	$2_{12}-1_{01}$
31 350.124	115	10	135			
31 350.717	128	11	133		117	$4_{14}-3_{03}$
level 31 362						
31 360.448	126	12	135		105	$2_{12}-3_{13}$
31 360.922	110	12	140		95	4_{04-413}
31 361.027					98	$1_{11}-2_{12}$
31 362.217	95	12	138		93	$2_{12}-2_{11}$
31 362.545	99	12	141		100	$1_{11}-2_{02}$
31 362.859	90	14	142		87	
31 363.416	91	12	138		96	$1_{01}-0_{00}$
31 364.019	101	12	136		108	$2_{02}-1_{01}$
31 365.244	109	12	136		110	$4_{04}-3_{03}$
31 365.776	102	12	139		103	$3_{13}-2_{02}$
31 366.993	102	12	135		99	$5_{15}-4_{04}$
31 367.033					102	
31 370.945	128	10	125			
level 31 527						
31 519.357	51		60		84	
31 520.275	66		63	3	100	
31 523.331	57		66		72	
31 523.575	38	10	77			
31 524.004	44	9	76	3	84	
31 524.559	38		62		115	$2_{02}-1_{01}$
31 524.620	40	10	66	≤2	64	$2_{12}-3_{13}$
31 525.216	54	9	71		78	$1_{11}-2_{12}$
31 525.270				<2	71	$3_{03}-2_{02}$
31 528.022	56	11	75		89	
31 528.664	52	11	72		98	$1_{11}-0_{00}$
31 529.329	53	10	72	4	82	
31 529.432	48		69	4	95	
31 529.918	51	10	70	≤2	82	$3_{13}-2_{02}$
31 532.228	60		68	3	107	
level 31 585						
31 590.167	21	10	40		53	$1_{11}-1_{10}$
31 592.404	23	9	46		46	$1_{11}-0_{00}$
31 593.054	26	11	45		48	
31 593.709	20	11	38		34	$3_{13}-2_{02}$

[a] A single time constant is listed for a fit to a single-exponential function. [b] Decay with large oscillatory modulation.

plane bend) promote decay of S_1. Future work in vibrational assignments in this region is expected to elucidate these experimental results.

2. Appearance of Fragment HCO at Medium Resolution. The appearance of HCO was detected at several levels to compare with the results from decay of initially prepared states. Two experimental curves for vibrational levels at 31 362 and 31 527 cm^{-1} are shown in Figure 4. Because the molecular jet with a warmer rotational temperature was used to measure the rise of fragment HCO, within the laser frequency profile many transitions possibly containing states with high J are excited. For bands at 31 346 and 31 527 cm^{-1}, spectra recorded with high and medium resolution are shown in Figure 8 for comparison. The yield of total fluorescence of fragment HCO appears to rise single-exponentially because states $\tilde{A}^1A''$ (S_1) and T_1 mix strongly; the appearance of products is expected to correspond to population decay of S_1/T_1 eigenstates. Even for decay of excited states of acetaldehyde displaying strong oscillatory modulation obtained with medium resolution, the appearance of HCO under similar experimental conditions shows a smooth single-exponential rise.

The time constant of HCO rise and of decay of parent excited states obtained at medium resolution are listed in Table 1. The time constant for decay of nearby excited states at high resolution is listed for comparison; the assignments are made according to the transitions to bright states. In Figure 9 the time constant is plotted versus excitation energy. For a vibrational level at 31 362 cm^{-1} the time constants for decay of individual rotational states are in general slightly larger than those measured with high resolution whereas the other three levels display smaller constants. This is because some states with high J were photolyzed, consistent with results from high-resolution work, i.e., mixing with more states with short lifetime results in small time constant when detected with medium resolution. For the level at 31 362 cm^{-1} the coupling states have long lifetimes, with a warm jet the average lifetime is expected to be long.

For all four vibrational levels the time constants of appearance of HCO are on average smaller than the decay constants obtained for the same wavelengths under similar conditions. This deviation becomes increasingly significant as excitation energy increases. In the case of deuterated acetaldehyde, large

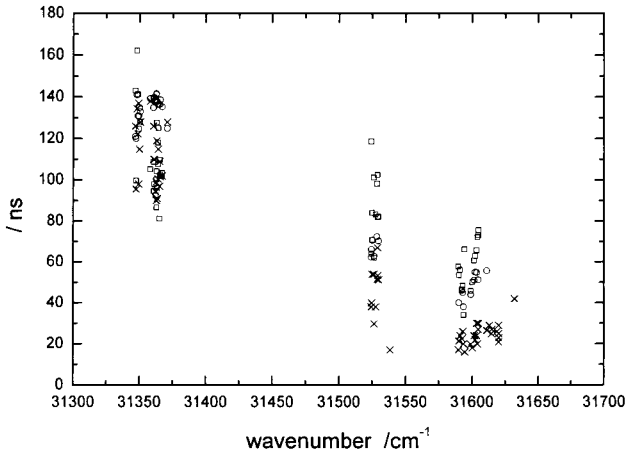

Figure 9. Plot of lifetime of decay of $\tilde{A}^1A''$ state at high (□) and medium (○) resolution and time constant of HCO rise (×) recorded with medium-resolution laser vs excitation energy for these four vibrational levels.

deviation is observed as excitation energy exceeds the top of the dissociation barrier.[37] A similar deviation is reported for dissociation of NO_2 in its ground electronic surface.[10e] This is because part of the mixed S_1/T_1 states (initially prepared eigenstates) is effectively coupled to dissociation. The fluorescence decay is attributed mainly to states that contain bright character (state $\tilde{A}^1A''$) but a product channel correlates to dark vibrational states of T_1 that couple to dissociation more effectively. The amount of energy may not be transferred effectively to dissociation coordinate when methyl torsion, inversion of aldehyde hydrogen, and C−C−O bending modes are excited; the progressions to those levels are most prominent at the low-energy region for the $\tilde{A}^1A''-\tilde{X}^1A'$ transition. For this reason we observed deviation between decay of parent molecule and appearance of fragments.

In the same laboratory we reported a systematic dependence of lifetime of the triplet state on rotational quantum number, indicating Coriolis-induced vibrational coupling of triplet states to dissociating continuum on the exit side of the dissociation barrier.[18] The lifetime of the triplet states is shorter as the rotational quantum numbers *J* and *K* increase. Under conditions of warmer jet and medium resolution, the states with high *J* were prepared that may lead the couple to dissociation effectively. One would expect that states with high *J* are coupled to more triplet states; a large deviation between the decay of eigenstates and appearance of fragment maybe expected. Current experimental results are insufficient to provide the information on the dependence of deviation on the rotational quantum number. Future work with high resolution on photolysis laser will provide more evidence in elucidating this issue.

In summary, we detected the lifetime of rovibrational levels of electronic state $\tilde{A}^1A''$ near a threshold for dissociation into radical fragments. The measured lifetimes vary with rotational quantum number resulting from increased number of T_1 states that couple to a given $\tilde{A}^1A''$ state. A rapid appearance of fragment HCO relative to fluorescence decay of initially prepared states of acetaldehyde indicates that excited states do not couple equally to the dissociation continuum. Before dissociation an incomplete vibrational redistribution among vibrational modes within the triplet manifold is observed.

Acknowledgment. C.-L.H., V.C., and I-C.C. thank the National Science Council of the Republic of China for financial support under contract No. NSC 88-2113-M-007-045. C.-K.N. and A.H.K. thank NSC, Republic of China, for support.

References and Notes

(1) Polik, W. F.; Guyer, D. R.; Moore, C. B. *J. Chem. Phys.* **1990**, *92*, 3453.
(2) Poilk, W. F.; Guyer, D. R.; Miller, W. H.; Moore, C. B. *J. Chem. Phys.* **1990**, *92*, 3471.
(3) Adamson, G. W.; Zhao, X.; Field, R. W. *J. Mol. Spectrosc.* **1993**, *160*, 11.
(4) Neyer, D. W.; Luo, X.; Burak, I.; Houston, P. L. *J. Chem. Phys.* **1995**, *102*, 1645.
(5) Tobiason, J. D.; Dunlop, J. R.; Rohlfing, E. A. *J. Chem. Phys.* **1995**, *103*, 1448.
(6) Stöck, C.; Li, X. N.; Keller, H.-M.; Schinke, R.; Temps, F. *J. Chem. Phys.* **1997**, *106*, 5333.
(7) Keller, H. M.; Stumpf, M.; Schroder, F.; Stöck, C.; Temps, F.; Schinke, R.; Werner, H. J.; Bauer, C.; Rosmus, P. *J. Chem. Phys.* **1997**, *106*, 5359.
(8) Choi, Y. S.; Moore, C. B. *J. Chem. Phys.* **1992**, *97*, 1010.
(9) Choi, Y. S.; Moore, C. B. In *Molecular Dynamics and Spectroscopy by Stimulated Emission Pumping*; Dai, H.-L., Field, R. W., Eds.; World Scientific: Singapore, 1995; p 433.
(10) (a) Miyawaki, J.; Yamanouchi, K.; Tsuchiya, S. *J. Chem. Phys.* **1993**, *99*, 254. (b) Reid, S. A.; Brandon, J. T.; Hunter, M.; Reisler, H. *J. Chem. Phys.* **1993**, *99*, 4860. (c) Reid, S. A.; Robie, D. C.; Reisler, H. *J. Chem. Phys.* **1994**, *100*, 4256. (d) Reid, S. A.; Reisler, H. *J. Chem. Phys.* **1994**, *101*, 5683. (e) Abel, B.; Hamann, H. H.; Lange, N. *Faraday Discuss. Chem. Soc. London* **1995**, *102*, 147.
(11) Geers, A.; Kappert, J.; Temps, F.; Wiebrecht, J. *J. Chem. Phys.* **1993**, *99*, 2271.
(12) Dertinger, S.; Geers, A.; Kappert, J.; Wiebrecht, J.; Temps, F. *Faraday Discuss. Chem. Soc. London* **1995**, *102*, 31.
(13) Wedlock, M. R.; Jost, R.; Rizzo, T. R. *J. Chem. Phys.* **1997**, *107*, 10344.
(14) Callegari, A.; Rebstein, J.; Muenter, J. S.; Jost, R.; Rizzo, T. R. *J. Chem. Phys.* **1999**, *111*, 123.
(15) Lee, S.-H.; Chen, I-C. *J. Chem. Phys.* **1996**, *105*, 4597.
(16) Lee, S.-H.; Chen, I-C. *Chem. Phys.* **1997**, *220*, 175.
(17) Gejo, T.; Bitto, H.; Huber, J. R.*Chem. Phys. Lett.* **1996**, *261*, 443.
(18) Huang, C.-L.; Chien, V.; Chen, I-C.; Ni, C. K.; Kung, A. H. *J. Chem. Phys.* **2000**, *112*, 1797.
(19) Jen, S.-H.; Hsu, T.-J.; Chen, I-C. *Chem. Phys.* **1998**, *232*, 131.
(20) Ni, C. K.; Kung, A. H. *Opt. Lett.* **1996**, *21*, 1673.
(21) Ni, C. K.; Kung, A. H. *Appl. Opt.* **1998**, *37*, 530.
(22) Noble, M.; Apel, E. C.; Lee, E. K. C. *J. Chem. Phys.* **1983**, *78*, 2219.
(23) Noble, M.; Lee, E. K. C. *J. Chem. Phys.* **1984**, *81*, 1632.
(24) Baba, M.; Hanazaki, I.; Nagashima, U. *J. Chem. Phys.* **1985**, *82*, 3938.
(25) Price, J. M.; Mack, J. A.; Helden, G. V.; Yang, X.; Wodtke, A. M. *J. Phys. Chem.* **1994**, *98*, 1791.
(26) Weersink, R. A.; Cramb, D. T.; Wallace, S. C.; Gordon, R. D. *J. Chem. Phys.* **1995**, *102*, 623.
(27) Liu, H.; Lim, E. C.; Judge, R. H.; Moule, D. C. *J. Chem. Phys.* **1995**, *102*, 4315.
(28) Liu, H.; Lim, E. C.; Muñoz-Caro, C.; Niño, A.; Judge, R. H.; Moule, D. C. *J. Mol. Spectrosc.* **1996**, *175*, 172.
(29) Liu, H.; Lim, E. C.; Niño, A.; Muñoz-Caro, C.; Judge, R. H.; Moule, D. C. *J. Mol. Spectrosc.* **1998**, *190*, 78.
(30) Lahmani, F.; Tramer, A.; Tric, C. *J. Chem. Phys.* **1974**, *60*, 4431.
(31) Frad, A.; Lahmani, F.; Tramer, A.; Tric, C. *J. Chem. Phys.* **1974**, *60*, 4419.
(32) Van Der Werf, R.; Schutten, E.; Kommandeur, J. *Chem. Phys.* **1975**, *11*, 281.
(33) Van Der Werf, R.; Schutten, E.; Kommandeur, J. *Chem. Phys.* **1976**, *16*, 151.
(34) Van Der Werf, R.; Zevenhuijzen, D.; Kommandeur, J. *Chem. Phys. Lett.* **1974**, *27*, 325.
(35) Van Der Werf, R.; Kommandeur, J. *Chem. Phys.* **1976**, *16*, 125.
(36) Leu, G.-H.; Huang, C.-L.; Lee, S.-H.; Lee, Y.-C.; Chen, I.-C. *J. Chem. Phys.* **1998**, *109*, 9340.
(37) Abou-Zied, O. K.; McDonald J. D. *J. Chem. Phys.* **1998**, *109*, 1293.
(38) Noble, M.; Lee, E. K. C. *J. Chem. Phys.* **1984**, *80*, 134.